

Technical Reference on Hydrogen Compatibility of Materials

Low-Alloy Ferritic Steels: Tempered Fe-Cr-Mo Alloys (code 1211)

Prepared by:
B.P. Somerday, Sandia National Laboratories

Editors
C. San Marchi
B.P. Somerday
Sandia National Laboratories

This report may be updated and revised periodically in response to the needs of the technical community; up-to-date versions can be requested from the editors at the address given below or downloaded at <http://www.ca.sandia.gov/matlsTechRef/>. The success of this reference depends upon feedback from the technical community; please forward your comments, suggestions, criticisms and relevant public-domain data to:

Sandia National Laboratories
Matls Tech Ref
B.P. Somerday (MS-9402)
7011 East Ave
Livermore CA 94550.

This document was prepared with financial support from the Safety, Codes and Standards program element of the Hydrogen, Fuel Cells and Infrastructure program, Office of Energy Efficiency and Renewable Energy; Pat Davis is the manager of this program element. Sandia is a multiprogram laboratory operated by Sandia Corporation, a Lockheed Martin Company, for the United States Department of Energy under contract DE-AC04-94AL85000.

IMPORTANT NOTICE

WARNING: Before using the information in this report, you must evaluate it and determine if it is suitable for your intended application. You assume all risks and liability associated with such use. Sandia National Laboratories make NO WARRANTIES including, but not limited to, any Implied Warranty or Warranty of Fitness for a Particular Purpose. Sandia National Laboratories will not be liable for any loss or damage arising from use of this information, whether direct, indirect, special, incidental or consequential.

1. General

Carbon and alloy steels can be categorized by a variety of characteristics such as composition, microstructure, strength level, material processing, and heat treatment [1]. The carbon and alloy steel categories selected for the Technical Reference for Hydrogen Compatibility of Materials are based on characteristics of the steels as well as available data. In this chapter, the steels are distinguished by the primary alloying elements, i.e., chromium (< 2.5 wt%) and molybdenum (< 1.25 wt%). Additionally, data in this chapter pertain to steels that were heat treated by heating in the austenite phase field (austenitizing), cooling, then tempering at intermediate temperatures to achieve the final mechanical properties. Hydrogen compatibility data exist primarily for the following Cr-Mo steels: 4130, 4140, 4145, 4147, and 2.25Cr-1Mo. Since a full range of data is not available for each steel, data for all Cr-Mo steels are presented in this chapter. Although the steels exhibit some metallurgical differences, many of the data trends are expected to apply to each steel.

The Cr-Mo steels are attractive structural materials in applications such as pressure vessels because of combinations of strength and toughness that can be achieved through tempering. However, the tempered Cr-Mo steels must be used judiciously in structures exposed to hydrogen gas. Hydrogen gas degrades the tensile properties of Cr-Mo steels, particularly in the presence of stress concentrations. Additionally, hydrogen gas lowers fracture toughness and renders the steels susceptible to crack extension under static loading. Hydrogen gas also accelerates fatigue crack growth. The severity of these manifestations of hydrogen embrittlement depends on material and environmental variables. Important variables include yield strength, hydrogen gas pressure, and temperature. Control over these variables individually or in combination may allow Cr-Mo steels to be applied safely in hydrogen gas environments. For example, limiting steel yield strength can improve resistance to hydrogen embrittlement.

This chapter emphasizes fracture mechanics properties, since pressure vessel design codes employ defect-tolerant design principles, particularly for hydrogen environments. Not all fracture mechanics data for Cr-Mo steels have been generated for material and environmental conditions that reflect conditions anticipated for applications in a hydrogen energy infrastructure. For example, some data pertain to high-strength steels exposed to low hydrogen gas pressures. In these cases, the data can provide insight into trends for Cr-Mo steels exposed to hydrogen gas, but the data are not intended for use in calculating design margins. Additional materials testing is needed to assure that hydrogen compatibility data are obtained for the specific combination of mechanical, material, and environmental variables required in any given application.

1.1 Composition, heat treatment, and mechanical properties

Table 1.1.1 lists the allowable composition ranges for Cr-Mo steels covered in this chapter. Table 1.1.2 summarizes the compositions of steels from hydrogen compatibility studies reported in this chapter. Table 1.1.3 details the heat treatments applied to steels in Table 1.1.2. Additionally, Table 1.1.3 includes the yield strength, ultimate tensile strength, reduction of area, and fracture toughness that result from the heat treatments.

1.2 Steel common names and selected specifications

4130: UNS G41300, AISI 4130, AMS 6370, ASTM A29 (4130), SAE J404 (4130)

4140: UNS G41400, AISI 4140, AMS 6382, ASTM A29 (4140), SAE J404 (4140)

4145: UNS G41450, AISI 4145, ASTM A29 (4145), SAE J404 (4145)

4147: UNS G41470, AISI 4147, ASTM A29 (4147)

2.25Cr-1Mo: UNS K21590, ASTM A335 (P22)

2. Permeability

The permeability of 4130 to hydrogen gas (0.01 to 3 MPa pressure) was measured over the temperature range 373 to 873 K [2]. Permeation was measured for two conditions of 4130: normalized (ferrite + carbide microstructure) as well as quenched and tempered (martensitic microstructure). The temperature dependence of permeability (ϕ) was reported as [2]:

Normalized 4130

$$\phi = 2.91 \times 10^{-5} \frac{\text{mol H}_2}{\text{m} \cdot \text{s} \cdot \sqrt{\text{MPa}}} \exp \left(\frac{-39.7 \frac{\text{kJ}}{\text{mol}}}{RT} \right)$$

Quenched and tempered 4130

$$\phi = 3.64 \times 10^{-5} \frac{\text{mol H}_2}{\text{m} \cdot \text{s} \cdot \sqrt{\text{MPa}}} \exp \left(\frac{-35.2 \frac{\text{kJ}}{\text{mol}}}{RT} \right)$$

3. Mechanical Properties: Effects of Gaseous Hydrogen

3.1 Tensile properties

3.1.1 Smooth tensile properties

Measurement of smooth tensile properties of 4140 in high-pressure hydrogen gas demonstrates that hydrogen severely degrades reduction of area but not ultimate tensile strength. Table 3.1.1.1 shows that reduction of area measured in high-pressure hydrogen gas is 80% lower compared to the measurement in high-pressure helium gas [3].

3.1.2. Notched tensile properties

High-pressure hydrogen significantly reduces tensile strength in 4140 when measurements are conducted using notched specimens. In addition, the yield strength of 4140 dictates the severity of tensile strength degradation measured from notched specimens. Table 3.1.2.1 shows that tensile strength is 60% lower in hydrogen compared to the value in helium for high-strength 4140 [3]. For low-strength 4140, tensile strength is 15% lower in hydrogen.

The absolute reduction of area measured in hydrogen gas depends on the yield strength of 4140. Table 3.1.2.1 shows that reductions of area are 0.9% and 7.1% for high-strength and low-strength 4140, respectively. Hydrogen lowers reduction of area by 70% and 50% compared to values in helium for high-strength and low-strength 4140, respectively.

Walter and Chandler [3, 4] categorized the hydrogen embrittlement susceptibility of materials tested in high-pressure hydrogen gas based on the reduction of tensile strength for notched specimens and the reduction of ductility for both notched and smooth specimens. The four categories of embrittlement were as follows: extreme, severe, slight, and negligible. The high-strength 4140 was classified as extremely embrittled [3, 4].

3.2 Fracture mechanics

3.2.1 Fracture toughness

The fracture toughness of 2.25Cr-1Mo in hydrogen gas (K_{IH}) is significantly lower than the fracture toughness in argon (K_{Ic}). Table 3.2.1.1 shows that K_{IH} is about 75% lower than K_{Ic} for hydrogen gas pressures between 1 and 10 MPa [5].

3.2.2 Threshold stress-intensity factor

The critical stress-intensity factor for hydrogen-assisted crack extension under static loading is termed a threshold (i.e., K_{TH}). Values of K_{TH} are sensitive to material and environmental variables. The trends in K_{TH} as a function of these variables are described below.

Effect of yield strength

Yield strength is a critical material variable governing K_{TH} . Increasing yield strength can dramatically lower K_{TH} [6-9], as demonstrated in Figure 3.2.2.1 for 4130 tested in low-pressure (0.08 MPa) hydrogen gas. The K_{TH} values decrease by a factor of three as yield strength increases in the range 1050 to 1330 MPa.

The dominant effect of yield strength is also observed for steels tested in high-pressure hydrogen gas [8]. Table 3.2.2.1 summarizes K_{TH} values for 4130, 4145, and 4147 in high-pressure (21 to 97 MPa) hydrogen gas. The K_{TH} for 4145 measured in 21 and 41 MPa hydrogen gas decreases by more than a factor of three as steel yield strength increases from 670 to 1055 MPa. Similarly, K_{TH} for 4147 measured in 21 to 97 MPa hydrogen gas decreases by a factor of two to three as yield strength increases from 725 to 870 MPa.

Effect of gas pressure

Hydrogen gas pressure is a critical environmental variable governing K_{TH} . The prevailing trend is that K_{TH} decreases as gas pressure increases. This trend is demonstrated from the K_{TH} vs gas pressure plots constructed for 4130 steel (1330 MPa yield strength) at three temperatures in Figure 3.2.2.2 [6, 7]. The K_{TH} is less sensitive to gas pressure as the pressure increases. The plots are shifted to higher K_{TH} values as temperature increases.

The K_{TH} vs gas pressure trends are influenced by material yield strength (Table 3.2.2.1) [8]. The K_{TH} for low-strength ($S_y = 670$ MPa) 4145 decreases by a factor of two as hydrogen gas pressure increases from 21 to 97 MPa. In contrast, K_{TH} values for high-strength ($S_y = 1055$ MPa) 4145 are nearly constant at gas pressures of 21 and 41 MPa. Additionally, the K_{TH} for low-strength ($S_y = 725$ MPa) 4147 decreases by a factor of two as hydrogen gas pressure increases from 21 to 97 MPa. The K_{TH} for high-strength ($S_y = 870$ MPa) 4147 decreases by a smaller degree (40%) in the same gas pressure range. As described previously, absolute values of K_{TH} decrease as yield strength increases for all gas pressure ranges.

Effect of temperature

Both elevated and sub-ambient temperatures can significantly affect K_{TH} . Measurements in low-pressure hydrogen gas show that K_{TH} increases by 40 to 50% in 4130 at two yield strength levels

as absolute temperature increases 50 K above ambient (Figure 3.2.2.3) [6, 7]. The K_{TH} decreases by 25 to 30% as temperature decreases 70 K below ambient.

3.3 Fatigue

3.3.1 Low-cycle fatigue

No known published data in hydrogen gas.

3.3.2 Fatigue crack propagation

Hydrogen gas enhances the fatigue crack growth rate (da/dN). The effect of hydrogen gas on the crack growth rate *vs* stress-intensity factor range (ΔK) relationship for 2.25Cr-1Mo steel is demonstrated in Figure 3.3.2.1 [5]. The crack growth rates in hydrogen gas exceed those in argon gas at ΔK levels greater than 10 MPa \sqrt{m} . The ratio of crack growth rates in hydrogen and argon environments becomes more pronounced as ΔK increases. The fatigue crack growth rates are nearly insensitive to hydrogen gas pressures between 1 and 4 MPa.

The fatigue crack growth rate of 2.25Cr-1Mo steel in hydrogen gas is not a function of loading frequency from 0.05 to 1 Hz (Figure 3.3.2.2) [5]. The fatigue crack growth rate decreases by a factor of two as frequency increases to 5 Hz.

Additives to hydrogen gas can cause fatigue crack growth rates to increase or decrease. Figure 3.3.2.3 summarizes the effects of various additives on the fatigue crack growth rate of 2.25Cr-1Mo steel in hydrogen gas [5]. The results are reported as the ratio of the crack growth rate in hydrogen gas with a given additive and the crack growth rate in hydrogen gas only. The data show that O₂ and CO gas additives retard fatigue crack growth rates, while H₂O, CH₃SH and H₂S gas additives accelerate fatigue crack growth rates.

3.4 Creep

No known published data in hydrogen gas.

3.5 Impact

No known published data in hydrogen gas.

4. Fabrication

4.1 Properties of welds

The hydrogen compatibility of the heat-affected zone and fusion zone of welds must be considered. Performance of welds should not be gauged based on data for base metal.

5. References

1. "Classification and Designation of Carbon and Low-Alloy Steels", in *Metals Handbook, Properties and Selection: Irons, Steels, and High-Performance Alloys*, 10th ed., vol. 1, ASM International, Materials Park OH, 1990, pp. 140-194.
2. HG Nelson and JE Stein, "Gas-Phase Hydrogen Permeation Through Alpha Iron, 4130 Steel, and 304 Stainless Steel from Less Than 100 °C to Near 600 °C," NASA TN D-7265, NASA, Washington DC, 1973.

3. RJ Walter and WT Chandler, "Effects of High-Pressure Hydrogen on Metals in Ambient Temperatures Final Report," R-7780-1 (NASA contract NAS8-14), Rocketdyne, Canoga Park CA, 1969.
4. WT Chandler and RJ Walter, "Testing to Determine the Effect of High-Pressure Hydrogen Environments on the Mechanical Properties of Metals", in *Hydrogen Embrittlement Testing, ASTM STP 543*, ASTM, Philadelphia PA, 1974, pp. 170-197.
5. S Fukuyama and K Yokogawa, "Prevention of Hydrogen Environmental Assisted Crack Growth of 2.25Cr-1Mo Steel by Gaseous Inhibitors", in *Pressure Vessel Technology*, vol. 2, Verband der Technischen Überwachungs-Vereine, Essen, Germany, 1992, pp. 914-923.
6. HG Nelson and DP Williams, "Quantitative Observations of Hydrogen-Induced, Slow Crack Growth in a Low Alloy Steel," NASA TMX-62,253, NASA Ames Research Center, Moffett Field CA, 1973.
7. HG Nelson and DP Williams, "Quantitative Observations of Hydrogen-Induced, Slow Crack Growth in a Low Alloy Steel", in *Stress Corrosion Cracking and Hydrogen Embrittlement of Iron Base Alloys*, RW Staehle, J Hochmann, RD McCright, and JE Slater, eds., NACE, Houston TX, 1977, pp. 390-404.
8. AW Loginow and EH Phelps, "Steels for Seamless Hydrogen Pressure Vessels", *Corrosion*, vol. 31, 1975, pp. 404-412.
9. S Hinotani, F Terasaki, and K Takahashi, "Hydrogen Embrittlement of High Strength Steels in High Pressure Hydrogen Gas at Ambient Temperature", *Tetsu-To-Hagane*, vol. 64, 1978, pp. 899-905.
10. *Metals & Alloys in the Unified Numbering System*, Standard SAE HS-1086/2004, 10th ed., SAE International, Warrendale PA, 2004.

**Low-Alloy Ferritic Steels
Tempered**

Fe-Cr-Mo

Table 1.1.1. Allowable composition ranges (wt%) for Cr-Mo steels.*

Steel	Specification	Ref.	Cr	Mo	C	Mn	Si	P	S	Other
4130	UNS G41300	[10]	0.80 1.10	0.15 0.25	0.28 0.33	0.40 0.60	0.15 0.35	0.035 max	0.040 max	-
4140	UNS G41400	[10]	0.80 1.10	0.15 0.25	0.38 0.43	0.75 1.00	0.15 0.35	0.035 max	0.040 max	-
4145	UNS G41450	[10]	0.80 1.10	0.15 0.25	0.43 0.48	0.75 1.00	0.15 0.35	0.035 max	0.040 max	-
4147	UNS G41470	[10]	0.80 1.10	0.15 0.25	0.45 0.50	0.75 1.00	0.15 0.35	0.035 max	0.040 max	-
2.25Cr-1Mo	UNS K21590	[10]	2.00 2.50	0.90 max	0.15 0.60	0.30 max	0.50 max	0.030 max	0.030 max	-

*The total weight percent of elements listed does not add up to 100%; the balance for each steel is Fe.

Table 1.1.2. Compositions (wt%) of Cr-Mo steels in hydrogen compatibility studies.*

Steel	Ref.	Cr	Mo	C	Mn	Si	P	S	Other
4130 [†]	[2]	0.70	0.20	0.30	-	-	-	-	-
4140	[3]	0.93	0.20	0.40	0.83	0.31	0.009	0.014	-
2.25Cr-1Mo	[5]	2.46	0.94	0.12	0.50	0.03	-	0.008	-
4130 [†]	[6, 7]	1	0.2	0.30	-	-	-	-	-
4130	[8]	1.12	0.19	0.37	0.58	0.27	0.006	0.014	-
4145	[8]	0.85	0.17	0.46	0.85	0.27	0.009	0.025	-
4147	[8]	0.99	0.18	0.47	0.98	0.26	0.012	0.011	-

*The total weight percent of elements listed does not add up to 100%; the balance for each steel is Fe.

[†]nominal composition

Table 1.1.3. Heat treatments and mechanical properties of Cr-Mo steels in hydrogen compatibility studies.

Steel	Ref.	S _y (MPa)	S _u (MPa)	RA (%)	K _{IC} (MPa√m)	Heat Treatment
4140 (low strength)	[3]	642	745	68	-	A 1116 K/60 min + OQ + T 977 K/120 min + AC
4140 (high strength)	[3]	1235 [†]	1283 [†]	48 [†]	-	A 1116 K/60 min + WQ + T 755 K/120 min
2.25Cr-1Mo	[5]	430	555	-	206	A 1193 K/120 min + AC + T 963 K/1440 min
4130	[6, 7]	1050 1330	1140 1600	-	-	A 1116 K + WQ + (523 K < T < 813 K)/120 min
4130	[8]	635	820	67	125*	A 1144 K/120 min + OQ + T 908 K/120 min + AC
4145 (low strength)	[8]	670	895	57	153*	A 1144 K/60 min + OQ + T 866 K/60 min + AC
4145 (high strength)	[8]	1055	1130	54	114*	A 1116 K/30 min + WQ + T 839 K/60 min + AC
4147	[8]	725 870	905 1005	60 64	155 160*	A 1144 K/90 min + OQ + (905 K < T < 941 K)/60 min + AC

A = austenitize; AC = air cool; OQ = oil quench; T = temper; WQ = water quench

*not reported as standardized K_{IC} measurement

[†]properties measured in high-pressure helium gas

Table 3.1.1.1. Smooth tensile properties of Cr-Mo steels in high-pressure helium gas and high-pressure hydrogen gas at room temperature.

Steel	Ref.	Test Environment	Strain Rate (s^{-1})	S_y (MPa)	S_u (MPa)	El_t (%)	RA (%)
4140	[3]	69 MPa He 69 MPa H ₂	$3.3 \times 10^{-5}^*$	1235 [†] -	1283 1228	14 [‡] 2.6 [‡]	48 8.8

*strain rate up to S_y

[†]defined at deviation from linearity on load vs time plot

[‡]based on 32 mm gauge length

Table 3.1.2.1. Notched tensile properties of Cr-Mo steels in air, high-pressure helium gas and high-pressure hydrogen gas at room temperature.

Steel	Ref.	Specimen	Test Environment	Displacement Rate (mm/s)	S_y^* (MPa)	σ_s (MPa)	RA (%)
4140	[3]	(a)	air	$\sim 4 \times 10^{-4}$	642	1345	10
			69 MPa He		-	1259	14
			69 MPa H ₂		-	1074	7.1
4140	[3]	(a)	69 MPa He 69 MPa H ₂	$\sim 4 \times 10^{-4}$	1235	2160 862	2.8 0.9

*yield strength of smooth tensile specimen

(a) V-notched specimen: 60° included angle; minimum diameter = 3.81 mm; maximum diameter = 7.77 mm; notch root radius = 0.024 mm. Nominal stress concentration factor (K_t) = 8.4.

Table 3.2.1.1. Values of fracture toughness for Cr-Mo steel in hydrogen gas.

Steel	Ref.	S_y^{\dagger} (MPa)	RA [†] (%)	K_{Ic} (MPa \sqrt{m})	Test Environment	Displacement Rate (mm/s)	K_{IH} (MPa \sqrt{m})
2.25Cr- 1Mo	[5]	430	-	206	1.1 MPa H ₂	1.7x10 ⁻³	54
					4.0 MPa H ₂		52
					9.9 MPa H ₂		48

[†]yield strength and reduction of area of smooth tensile specimen in air

Table 3.2.2.1. Values of theshold stress-intensity factor for Cr-Mo steels at high hydrogen gas pressures.

Steel	Ref.	S_y^{\dagger} (MPa)	RA [†] (%)	K_{Ic} (MPa \sqrt{m})	Test Environment	K_{TH} (MPa \sqrt{m})
4130	[8]	635	67	125*	21 MPa H ₂	80
					41 MPa H ₂	62
					62 MPa H ₂	41
					69 MPa H ₂	29
					97 MPa H ₂	47
4145	[8]	670	57	153*	21 MPa H ₂	66
					41 MPa H ₂	61
					62 MPa H ₂	50
					69 MPa H ₂	55
					97 MPa H ₂	28
4145	[8]	1055	54	114*	21 MPa H ₂	20
					41 MPa H ₂	17
4147	[8]	725	64	155*	21 MPa H ₂	88
					41 MPa H ₂	85
					62 MPa H ₂	60
					97 MPa H ₂	42
4147	[8]	780	60	158*	21 MPa H ₂	112
					41 MPa H ₂	37
					62 MPa H ₂	41
					97 MPa H ₂	27
4147	[8]	870	61	160*	21 MPa H ₂	35
					41 MPa H ₂	27
					62 MPa H ₂	22
					97 MPa H ₂	21

[†]yield strength and reduction of area of smooth tensile specimen in air

*not reported as standardized K_{Ic} measurement

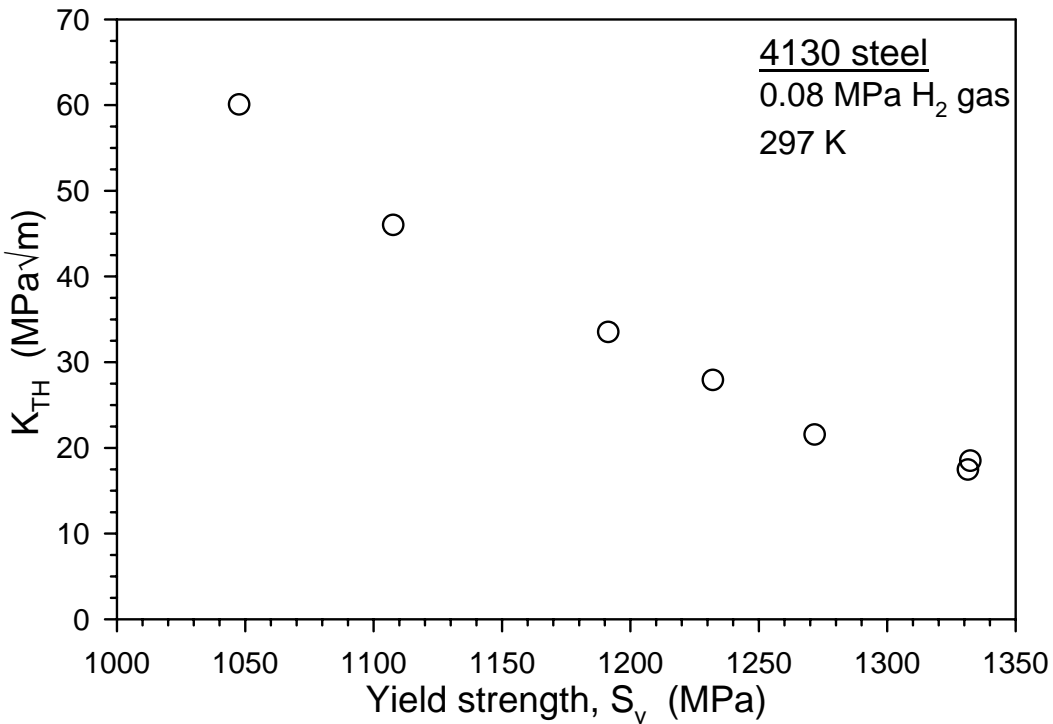


Figure 3.2.2.1. Effect of yield strength on threshold stress-intensity factor for crack extension in low-pressure hydrogen gas for 4130 steel [6, 7].

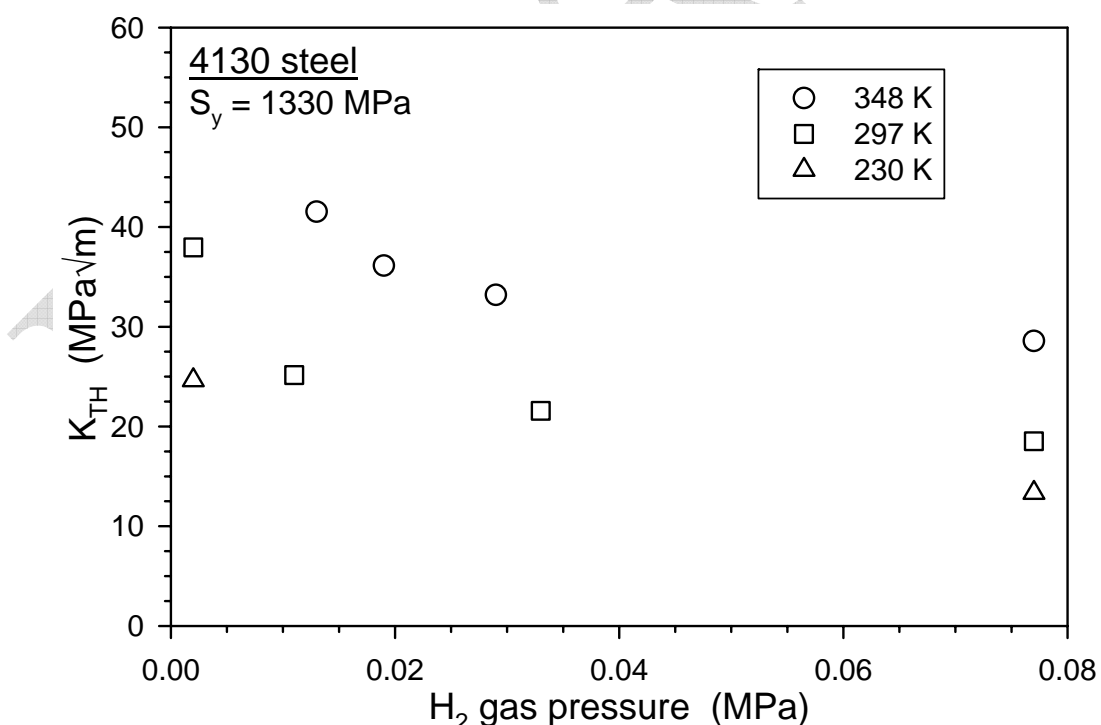


Figure 3.2.2.2. Effect of low hydrogen gas pressures on threshold stress-intensity factor for crack extension in high-strength 4130 steel [6, 7]. Results are shown for three temperatures.

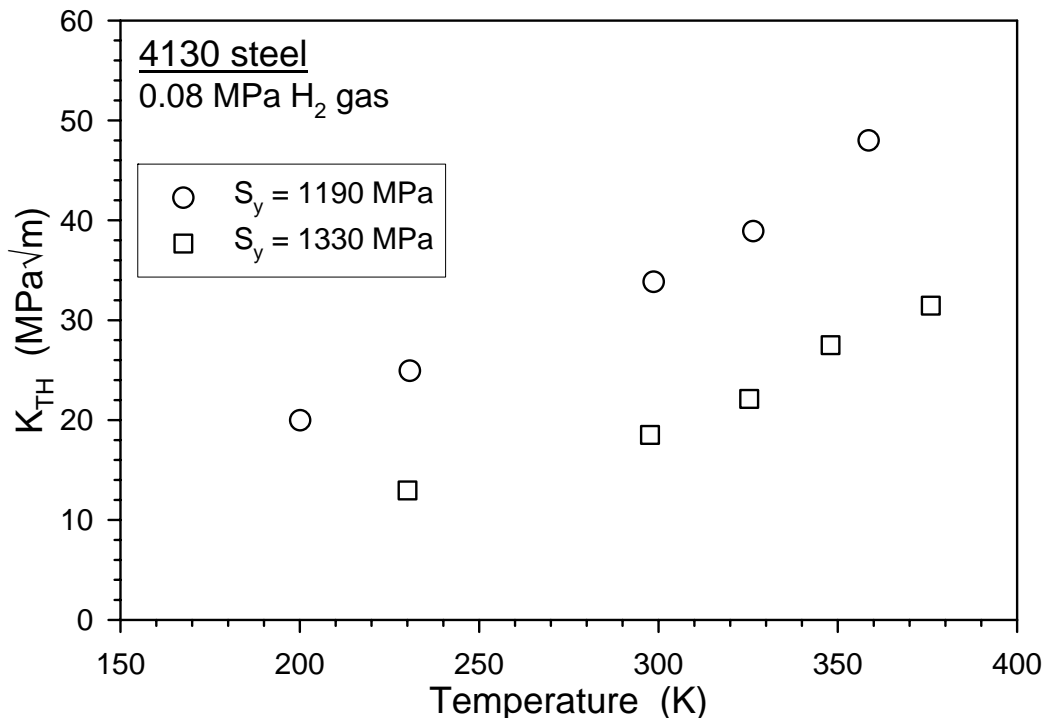


Figure 3.2.2.3. Effect of temperature on threshold stress-intensity factor for crack extension in low-pressure hydrogen gas for 4130 steel [6, 7]. Results are shown for two yield strengths.

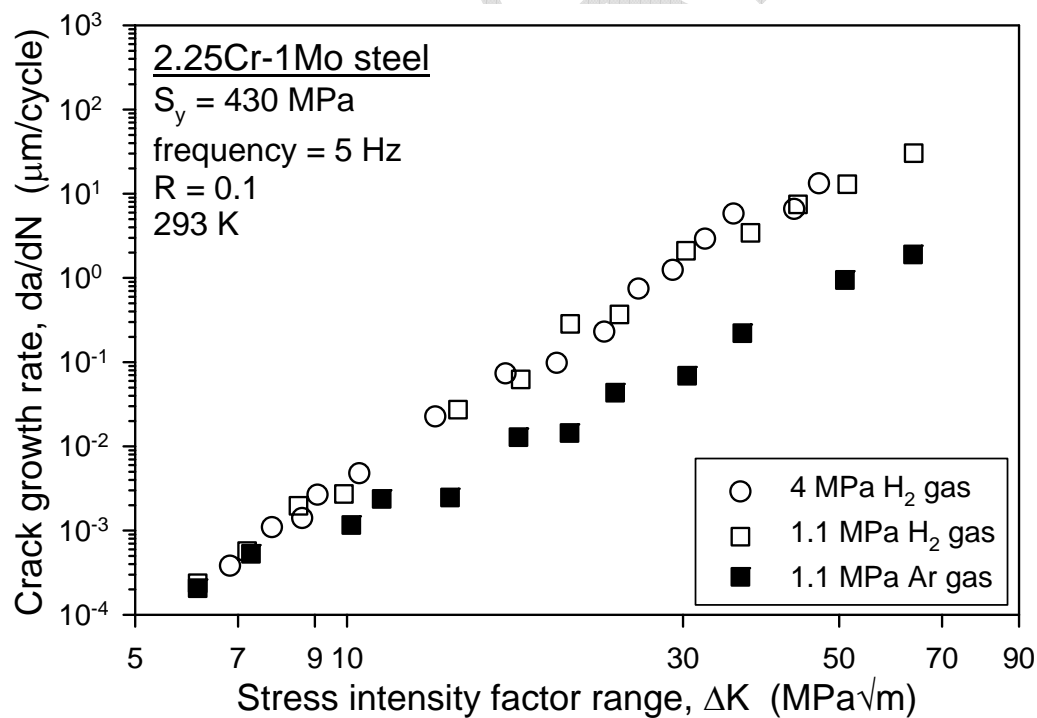


Figure 3.3.2.1. Fatigue crack growth rate as a function of stress-intensity factor range for 2.25Cr-1Mo steel in hydrogen and argon gases [5].

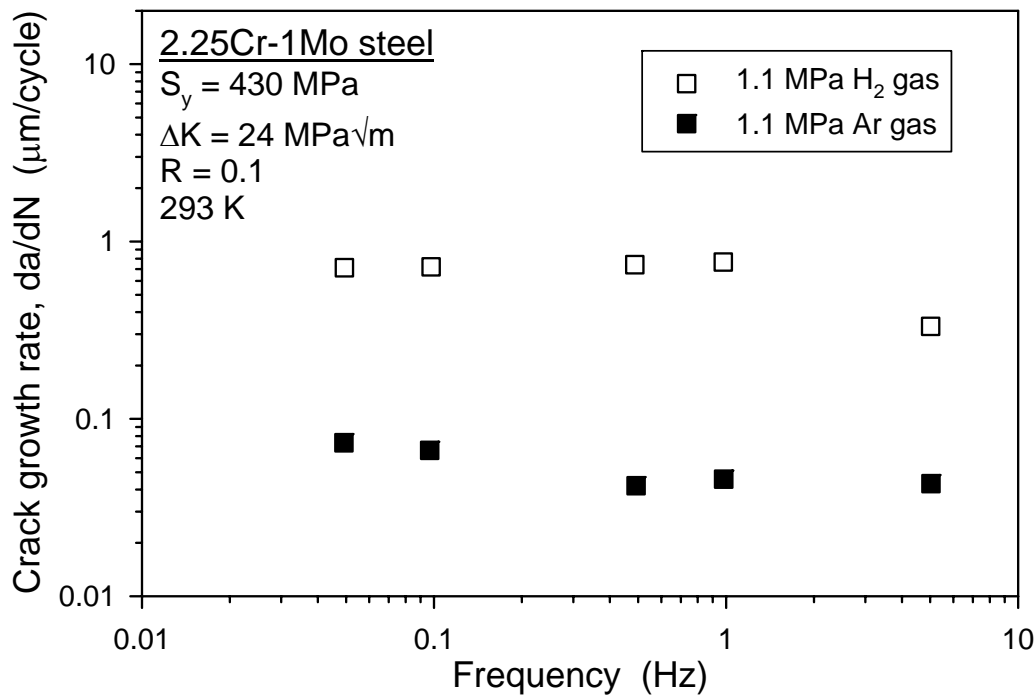


Figure 3.3.2.2. Fatigue crack growth rate as a function of load cycling frequency for 2.25Cr-1Mo steel at fixed stress-intensity factor range [5].

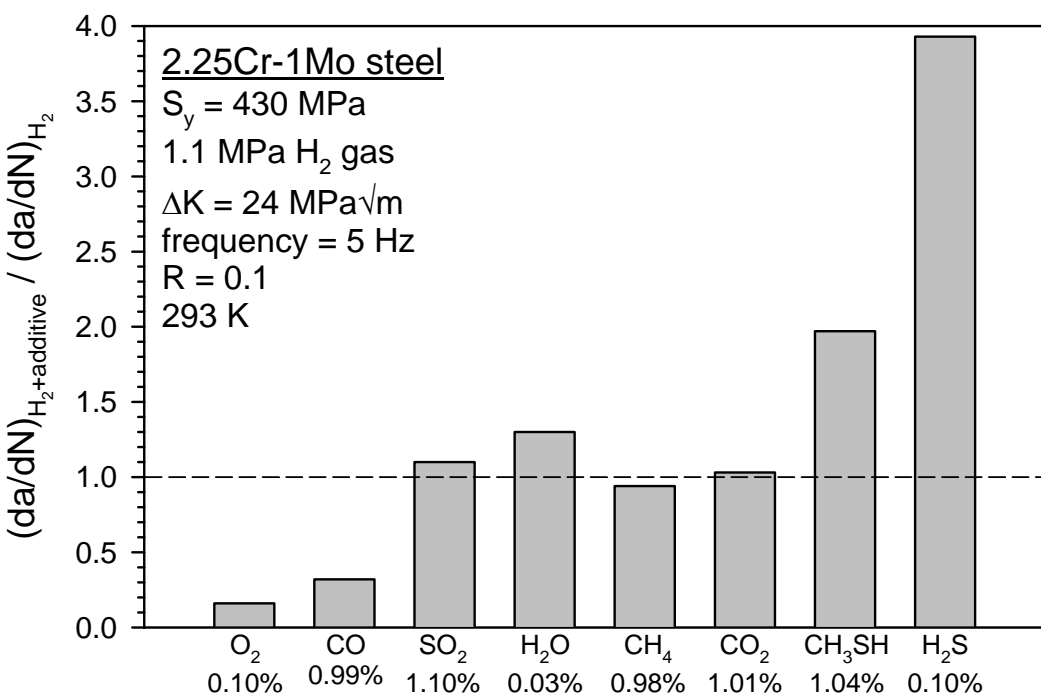


Figure 3.3.2.3. Ratio of fatigue crack growth rate in hydrogen gas with additives to fatigue crack growth rate in hydrogen gas at fixed stress-intensity factor range for 2.25Cr-1Mo steel [5].